

Primary and secondary crystallization processes of WSe₂ films

J. C. BERNEDE, S. BENHIDA

Faculté des Sciences et des Techniques, Laboratoire de Physique des Matériaux pour l'Electronique, 2, rue de la Houssinière, 44072 Nantes Cédex 02, France

WSe₂ thin films are obtained by annealing tungsten and selenium constituents in thin-film form, under selenium pressure. Thin films have been investigated by X-ray analysis, scanning and transmission electron microscopy, and by microprobe analysis. Annealing temperature and time were used as parameters. It is shown that stoichiometric thin films, crystallized in the hexagonal structure, are systematically obtained. The grain-size evolution with increasing temperature and/or annealing time is interpreted in terms of primary and second crystallization processes (crystallization and recrystallization).

1. Introduction

WSe₂ is a layer-type semiconductor with a band gap of 1.35 eV [1] which can be an efficient electrode in the realization of photoelectrochemical solar cells [2, 3]. In earlier papers [4, 5], we have described a process for obtaining stoichiometric textured WSe₂ thin films. The WSe₂ coatings were obtained by solid state reaction, induced by annealing under selenium pressure, between the tungsten and selenium constituents in thin-film form. It has been shown by X-ray diffraction and scanning electron microscope studies that the crystallite morphology depends on annealing time and temperature. In the present work, after a complementary study with electron microscopes (scanning and transmission), this evolution was interpreted in terms of recrystallization as developed by Thompson and co-workers [6, 7].

2. Experimental procedure

The deposition techniques have been described in earlier papers [4, 5]; they will be only briefly recalled here. Layers of tungsten and selenium were deposited sequentially, by sputtering of tungsten and evaporation of selenium. The number of layers varied from six to ten. The W/Se/W/.../Se structures were annealed in a vacuum-sealed glass tube at a temperature between 773 and 823 K for 72–168 h. The WSe₂ films were synthesized by solid-state reaction of the thin layers. The last amorphous selenium capping layer protects the tungsten films from oxidation during transfer from the deposition apparatus to the glass tube [8] and also permits annealing to be carried out under a small selenium pressure, which increases the quality of the films, as discussed in a preceding paper [5]. Therefore, during annealing, the last selenium layer was evaporated and the thicknesses of the other layers were calculated to achieve the desired composition, varying from 25–50 nm and from 90–775 nm for tungsten and selenium, respectively.

As shown earlier [4, 5], during the cooling of the glass tube, some selenium condensation takes place on the surface of the layers. This selenium excess is sublimed by annealing the samples under dynamic vacuum for 24 h at $T = 123$ K.

An X-ray diffractometer (XRD) using monochromatic CuK_α radiation was employed to obtain diffraction patterns from the films. Detailed morphological analysis of the films was carried out by scanning electron microscopy (SEM) using a Jeol 6400F field emission electron microscope. Another electron microscope equipped with a microprobe analyser, was used to check the composition of the films. Transmission electron microscopy (TEM) and electron diffraction were used to control the orientation, homogeneity; and morphology of the deposits. For examination in the TEM, the films were chemically removed from the glass substrates and then attached to copper grids.

3. Results

As shown by microprobe analysis, the films are stoichiometric. The results of XRD and SEM studies are shown in Figs 1–3. It can be seen that the grain size and the texture of the films increased with the time and/or temperature of annealing.

At 773 K after 72 h, small grains, about 100 nm in size, are embedded in less-crystallized matrix. The films show the beginning of (00 l) preferred orientation. However, peaks with other orientations are detected (Fig. 1a).

At the same temperature but after 168 h, the grain size has increased (a few 100 nm), and the badly crystallized matrix has disappeared. The crystallites have the (00 l) preferential orientation; however, the (002) ray is not detected and the relative intensities of the peaks, I/I_0 , are not in agreement with those of the ASTM data [9]. For the same duration when the annealing temperature is increased from 773 K to 823 K, the grain size is much higher (a few micrometres) and

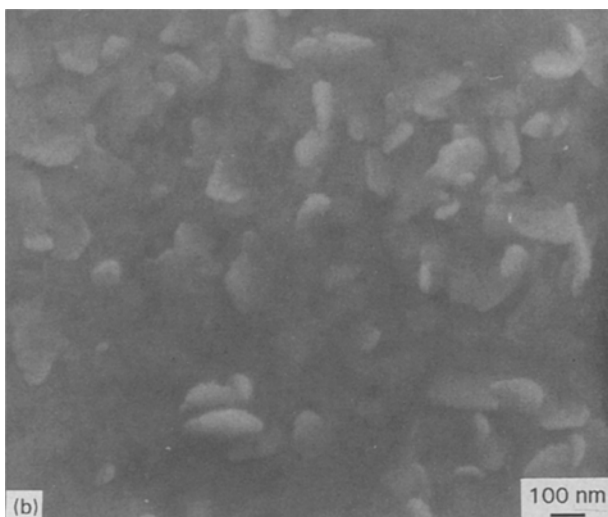
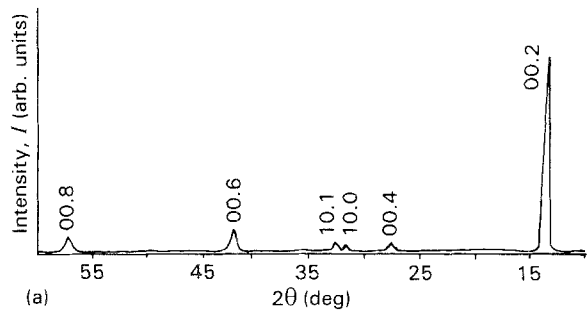


Figure 1 WSe₂ thin film after annealing at 773 K, 72 h: (a) XRD pattern, (b) scanning electron micrograph.

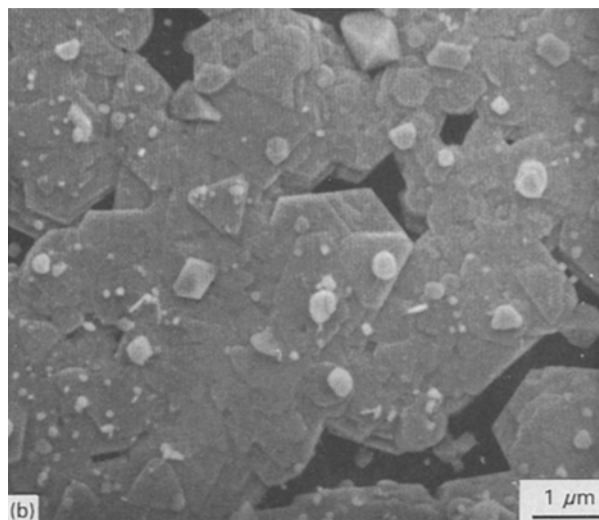
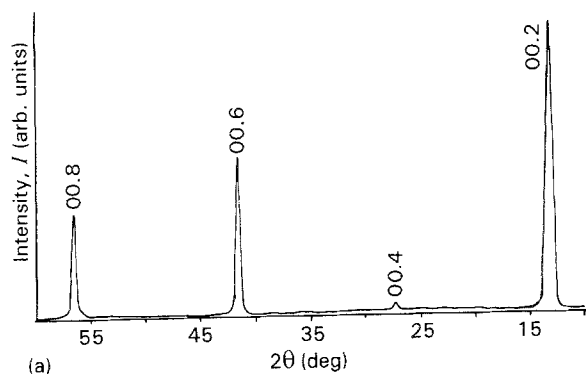


Figure 3 WSe₂ thin film after annealing at 823 K for 168 h: (a) XRD pattern, (b) scanning electron micrograph.

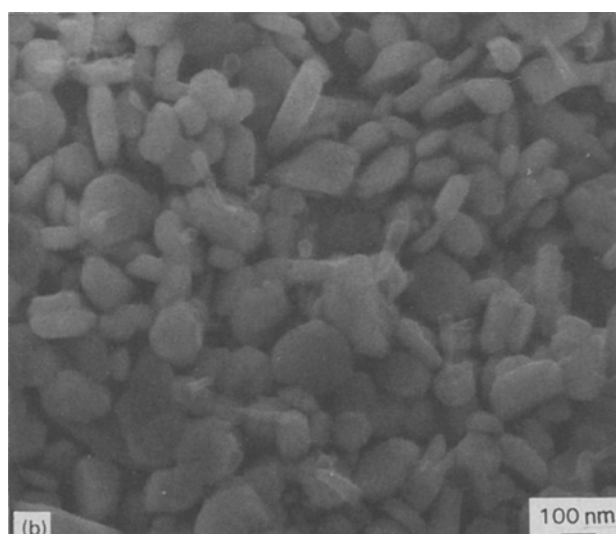
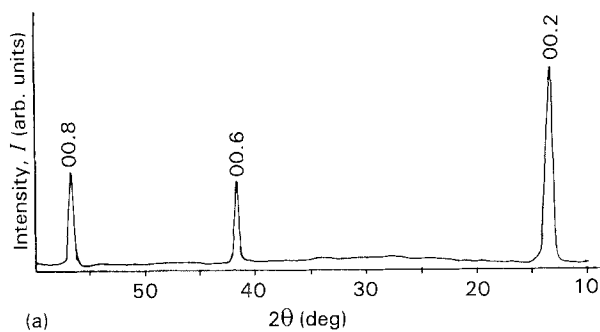


Figure 2 WSe₂ thin film after annealing at 773 K for 168 h: (a) XRD pattern, (b) scanning electron micrograph.

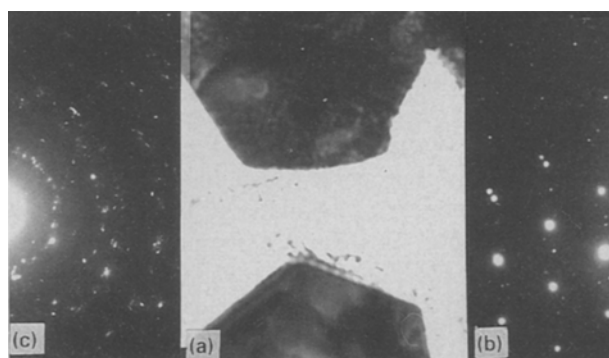


Figure 4 (a) Electron micrograph of a WSe₂ thin film after annealing at 823 K for 168 h; (b, c) electron diffraction patterns of regions 1 and 2 in the micrograph, respectively.

the XRD pattern is exactly that expected for a textured film with the *c*-axis perpendicular to the plane of the substrates. However, there are many pinholes in the films.

When visualized by TEM, these films exhibit very large, hexagonal-shaped crystallites (Fig. 4a). The electron diffraction pattern of these crystals confirms the fact that they have the hexagonal structure of WSe₂ (Fig. 4b) and that they have the *c*-axis perpendicular to the plane of the substrate. At the grain boundaries, the diffraction pattern (Fig. 4c) shows the existence of small badly oriented microcrystals of WSe₂.

4. Discussion

The evolution of the morphology of the crystallites will be discussed with the help of the model proposed by Thompson and co-workers [6, 7], who have shown that, after a polycrystalline film has been formed after deposition of an amorphous film and subsequent crystallization (primary crystallization), a subsequent recrystallization can occur. Recrystallization or secondary crystallization refers to a process in which new grains nucleate and grow within a pre-existing crystalline matrix.

Grain growth occurs in order to reduce the total energy of a solid. Therefore, grain growth is driven by the elimination of grain-boundary energy which accompanies the reduction in the total area of grain boundaries per unit volume. Thompson and co-workers demonstrated that, when the grain size is comparable to the film thickness, the energy of a grain includes not only the energy associated with the grain boundaries, but also the energy of the top surface and of the film substrate interface, therefore we have [6, 7]

$$\dot{r} = \frac{dr}{dt} = M \left[\frac{\gamma_s^* - \gamma_s}{h} + \frac{\gamma_i^* - \gamma_i}{h} + \gamma_{gb} \left(\frac{1}{\bar{r}} - \frac{1}{r} \right) \right] \quad (1)$$

where \dot{r} is the rate of growth of a grain, M the average grain-boundary mobility, h the thickness of the film, γ_s the surface energy of the growing grain, γ_s^* the average surface energy of the film, γ_i the energy of the film substrate interface, γ_i^* the average grain-boundary energy, \bar{r} the average grain radius, and r the radius of the grain under consideration.

Therefore, if the surface (interface) energy is a function of the crystallographic orientation of the grains, those grains with orientations that lead to low surface energies will grow faster than those grains with other orientations. The surface (interface) energy of a crystal is a fundamental property which depends on the nature of the bonding of the material [10]. The surface (interface) energy is the work required to separate a crystal into two parts along a plane and is equal to half the energy of cohesion. In the case of layer-type structure such as WSe_2 , the bonds between the planes perpendicular to the c -axis are Van der Waals bonds, while in the other directions the bonds are iono-covalents. Therefore, the surface energy of the planes perpendicular to the c -axis is far smaller than the others.

We have seen that at the onset of crystallization (Fig. 1), the crystallites are small and badly oriented, this may roughly correspond to the primary crystallization state. When the annealing time and/or temperature increases, there is a recrystallization process. As we have shown, γ is strongly dependent on the crystallographic orientation of a grain, this leads to preferred growth of the plane perpendicular to the c -axis. This

growth results in films composed of large grains, having the same plane parallel to the plane of the film, but random in plane orientations (Fig. 3), while all other grains which do not minimize γ , neither grow nor shrink. This process is visualized in Fig. 4 where we can see the large hexagonal grains grown during the recrystallization, while non-oriented microcrystallites remain at the grain boundaries. By comparison with the grain-size distribution proposed by Thompson [6], Fig. 4a shows that our films correspond to a picture situated between Fig. 2e and f of Ref. 6.

5. Conclusion

XRD, SEM and TEM studies describe the process of recrystallization well, as proposed by Thompson and co-workers, when the surface energy is strongly dependent on the crystallographic orientation of the grain, which is the case in layer-type WSe_2 .

Other metal dichalcogenides with the same hexagonal structure can be obtained in the textured thin-film form. $MoTe_2$ is very easy to obtain with the c -axis perpendicular to the plane of the substrate. The first state of crystallization has not been visualized, but this is only because the process is faster than with WSe_2 and we can imagine that $MoTe_2$ thin films follow the same process as that described here. In the laboratory we are now trying to obtain textured WSe_2 thin films without pinholes at the end of the recrystallization; for this, a better control of the process is required.

Acknowledgements

The authors thank Mr Barreau for performing the SEM measurements.

References

1. A. J. GRANT, J. A. WILSON and A. D. YOFFE, *Philos. Mag.* **25** (1972) 625.
2. H. TRIBUTSCH, *Solar Energy Mater.* **1** (1979) 257.
3. R. TENNE and A. WOLD, *Appl. Phys. Lett.* **47** (1985) 707.
4. S. BENHIDA, M. MORSLI, J. POUZET and J. C. BERNEDE, *Le vide, les couches minces* **261** (1992) 93.
5. S. BENHIDA, J. C. BERNEDE, J. POUZET and A. BARREAU, *Thin Solid Films* **224** (1993) 39.
6. C. V. THOMPSON, *J. Appl. Phys.* **58** (1985) 763.
7. C. V. THOMPSON, J. FLORO and H. I. SMITH, *ibid.* **67** (1990) 4099.
8. A. LATEF and J. C. BERNEDE, *Phys. Status Solidi A* **124** (1991) 243.
9. ASTM data file 38-1389 (American Society for Testing and Materials, Philadelphia, PA).
10. R. J. JACCODINE, *II Electrochem. Soc.* **110** (1963) 524.

Received 26 May

and accepted 16 December 1993